# In-Medium Isovector $\pi N$ Amplitude from Low-Energy Pion Scattering

E. Friedman,[1,*] M. Bauer,[2] J. Breitschopf,[2] H. Clement,[2] H. Denz,[2] E. Doroshkevich,[2] A. Erhardt,[2] G. J. Hofman,[3]
R. Meier,[2] G. J. Wagner,[2] and G. Yaari[1]

[1]*Racah Institute of Physics, The Hebrew University, Jerusalem 91904, Israel*
[2]*Physikalisches Institut, Universität Tübingen, 72076 Tübingen, Germany*
[3]*TRIUMF, Vancouver, British Columbia V6T2A3, Canada*
*and University of Regina, Regina, Saskatchewan S4S-0A2, Canada*
(Received 28 April 2004; published 16 September 2004)

Differential cross sections for elastic scattering of 21.5 MeV positive and negative pions by Si, Ca, Ni, and Zr have been measured as part of a study of the pion-nucleus potential across the threshold. The "anomalous" repulsion in the $s$-wave term was observed, as is the case with pionic atoms. The extra repulsion can be accounted for by a chiral-motivated model where the pion decay constant is modified in the medium. Unlike in pionic atoms, the anomaly cannot be removed by merely introducing an empirical on-shell energy dependence.

A long-standing "anomalous" $s$-wave repulsion in the pion-nucleus interaction at the threshold, as found in phenomenological analyses of strong interaction effects in pionic atoms, has recently received considerable attention [1–9] following the suggestion by Weise [1] that it could be expected, at least in the isovector channel, to result from a chirally motivated approach where the pion decay constant becomes density dependent in the nuclear medium. Very recently it was also argued [7,8] that the energy dependence of the chirally expanded $\pi N$ isoscalar and isovector amplitudes $b_0(E)$ and $b_1(E)$, respectively, for zero-momentum *off-shell* pions near the threshold, could explain the anomaly. In addition, the empirical *on-shell* energy dependence was shown in Ref. [9] to be capable of explaining the anomaly by imposing the minimal substitution requirement [10] of $E \rightarrow E - V_c$, where $V_c$ is the Coulomb potential, on the properly constructed pion optical potential used in a large-scale fit to 100 pionic-atom data across the periodic table. The availability in recent years of strong interaction level shifts and widths of "deeply bound" $1s$ and $2p$ pionic-atom states in isotopes of Pb and Sn [11–14], obtained from the $(d, {}^3\text{He})$ reaction, provides added impetus to the study of the $s$-wave pion-nucleus interaction at the threshold.

In the present Letter, we report on extending the study of the $s$-wave term of the pion-nucleus potential by measuring the elastic scattering of very low-energy $\pi^+$ and $\pi^-$ on several nuclei. The purpose of this experiment is to study the behavior of the pion-nucleus potential across the threshold into the scattering regime and to examine if the above-mentioned anomaly is observed also above the threshold. Of particular importance is the question of whether the density dependence or the empirical energy dependence, which remove the anomaly in pionic atoms, are required also by the scattering data. In the scattering scenario, unlike in the atomic case, one can study both charge states of the pion, thus increasing sensitivities to

isovector effects and to the energy dependence due to the Coulomb interaction.

It is somewhat surprising to realize that at kinetic energies well below 50 MeV there seems to be only one set of high quality data available for both charge states of the pion obtained in the same experiment, namely, the data of Wright *et al.* [15] for 19.5 MeV pions on calcium. Focusing attention on the isovector channel, it is desirable to include also nuclei with $N > Z$. Therefore the targets chosen for the present experiment, which was carried out at 21.5 MeV pion kinetic energy, were Si, Ca, Ni, and Zr, where the last two have an excess of neutrons. Natural isotopic mixtures have been used in all cases and have been taken into account in the model calculations accordingly.

The experiment was performed at 21.5 MeV pion energy on the piE3 channel at the Paul Scherrer Institute [16], using the high resolution low energy pion magnetic spectrometer (LEPS) [17]. Particles were identified by the time-of-flight relative to the HF signal of the cyclotron and by the time-of-flight within the spectrometer. Self-supporting targets were used in all cases. The beam was monitored by four decay-muon telescopes and by a downstream hodoscope [17]. The latter was also used to determine the beam composition and profile. The elastic scattering of muons with the same momentum as the pions (except for the different energy losses in material such as beam line and spectrometer windows and plastic scintillators) was used to calibrate the absolute scale of cross sections and to check the overall validity of data reduction. This was achieved by comparing the measured angular distributions for elastic scattering of muons with predictions made for Coulomb scattering from the known charge distributions of the target nuclei. Details on this method of muonic normalization, which has frequently been used for low-energy pion measurements with the LEPS spectrometer, can be found in Refs. [17,18]. Two

measurements of elastic scattering of muons were made for each measurement for pions: (i) Muons were recorded in parallel with pions but at a slightly different location in the focal plane, due to the different energy losses of muons and pions in the target and in the various scintillators. (ii) Muons were recorded in designated muon runs, where the spectrometer fields were adjusted to bring the muons to the same location in the focal plane as the pions in the proper pion runs. After correcting for effective target thickness and detector acceptance, we have obtained normalization constants common to all angles and to the two types of measurements (i) and (ii) mentioned above, but slightly different for $\mu^+$ and $\mu^-$, due to differences in the muon/pion ratios for the different beams. In this way, we could confirm the dependence of the acceptance of the spectrometer on the position in the focal plane, which was determined separately by scanning the magnetic fields.

Figure 1 shows as an example comparisons between calculations and measurements for the Coulomb scattering of muons by Ni. Open and solid symbols are for the two types of muon measurements (i) and (ii) mentioned above, respectively. The reliability of the focal-plane position dependence of the acceptance of LEPS is of major importance as the conclusions regarding the pion-nucleus interaction (see below) rely exclusively on the *shape* of the angular distributions. The points at 30° are not plotted because different normalizations apply due to different settings of the channel slits.

Figure 2 shows the experimental results for elastic scattering of pions and predictions of best-fit optical
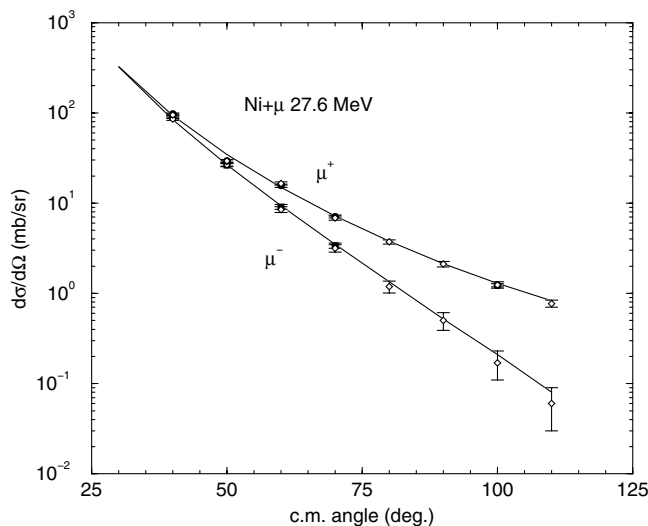


FIG. 1. Coulomb scattering of muons by Ni. Open symbols: from pion runs. Solid symbols: from designated muon runs. Continuous curves are calculated Coulomb scattering for the finite size charge distribution. Common normalization constants have been used separately for all the $\mu^+$ points and all the $\mu^-$ points; see text.

potentials. Before discussing the implications of $\chi^2$ fits, a comment on the values of errors is in order. (Full details of the experiment and the results will be published elsewhere.) The number of pion counts in the elastic scattering peaks was usually greater than 3000 and the background in the spectrometer was negligibly small, thus resulting in statistical errors of less than 2%. Most of the uncertainties in this experiment come from the monitoring of the beam intensity and its composition and from the dependence of the acceptance of the spectrometer on the position in the focal plane. The measurements with muons provided stringent tests of the latter, and careful analysis did not reveal any systematic effects. An estimated overall normalization error of 5% was given in [18]. For the purpose of $\chi^2$ fits we have added 5% in quadrature to the statistical errors for each point individually, but in order to check the dependence of the derived parameter values on the errors we have repeated the $\chi^2$ fits also for only 3% added in quadrature. Values of fit parameters and, in particular, values of the isovector amplitude $b_1$, which is at the focus of the present work, did not differ between fits made with these two sets of errors.

The interaction of pions with the target nuclei was described by the Klein-Gordon equation with the standard potential due to Ericson and Ericson [19] where double scattering, absorption on two nucleons, and angle-transformation terms have been included [6,20]. The potential is written as

$$2\mu V_{\mathrm{opt}}(r) = q(r) + \vec{\nabla} \cdot \alpha(r)\vec{\nabla} \tag{1}$$

with its *s*-wave term, which is the prime concern in the present work, given by

$$q(r) = -4\pi\left(1 + \frac{\mu}{M}\right)\{\bar{b}_0(r)[\rho_n(r) + \rho_p(r)] \pm b_1[\rho_n(r)$$
$$-\rho_p(r)]\} - 4\pi\left(1 + \frac{\mu}{2M}\right)4B_0\rho_n(r)\rho_p(r), \tag{2}$$

where the $\pm$ sign refers to the pion $\mp$ charge states, respectively. In these expressions, $\rho_n$ and $\rho_p$ are the neutron and proton density distributions normalized to the number of neutrons $N$ and number of protons $Z$, respectively, $\mu$ is the pion-nucleus relativistic reduced mass, and $M$ is the mass of the nucleon. The function $\bar{b}_0(r)$ in Eq. (2) is given in terms of the *local* Fermi momentum $k_F(r)$ corresponding to the isoscalar nucleon density distribution:

$$\bar{b}_0(r) = b_0 - \frac{3}{2\pi}(b_0^2 + 2b_1^2)k_F(r), \tag{3}$$

where $b_0$ and $b_1$ are the pion-nucleon isoscalar and isovector effective scattering amplitudes, respectively. The parameter $B_0$ represents *s*-wave absorption on pairs of nucleons. The expressions for the *p*-wave term are given in Refs. [6,20] and will not be given explicitly here, except
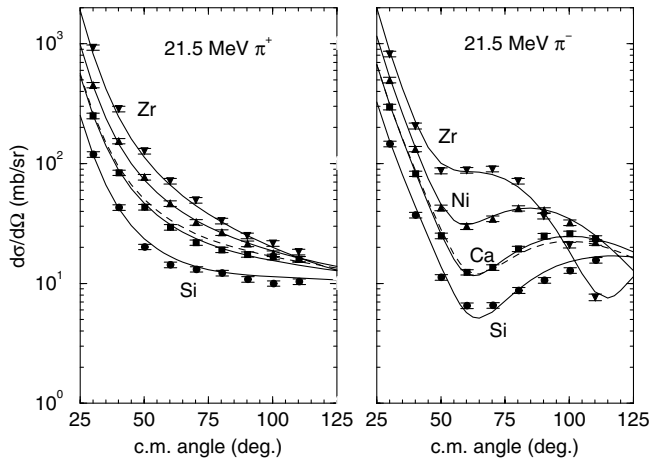
FIG. 2. Comparisons between experimental and calculated differential cross sections for elastic scattering of pions. Solid lines are for the best-fit optical potential (c′) of Table I; dashed lines are examples for potential (a′) (see text).

for its linear part, namely,

$$\alpha(r) = 4\pi\left(1 + \frac{\mu}{M}\right)^{-1}\{c_0[\rho_n(r) + \rho_p(r)] \pm c_1[\rho_n(r) - \rho_p(r)]\} + \text{quadratic terms.} \quad (4)$$

Nuclear densities were obtained from charge densities and using for the difference between neutron and proton rms radii either the results of relativistic mean field calculations or values obtained from antiprotonic atoms; see Ref. [6] for details. Derived values of $b_1$ were insensitive to assumptions on $\rho_n$ within those limits.

First attempts at parameter fits to the data using the above potential ran into difficulties which could be traced to the two-nucleon absorption in the $p$-wave term. Subsequent fits to the $\pi^+$ data and the $\pi^-$ data separately revealed the need to make the $p$-wave absorption parameter for $\pi^-$ considerably larger than the corresponding parameter for $\pi^+$, an effect not seen in earlier fits to only $\pi^-$ data [21]. This may be expected at 20 MeV since the effects of the (3,3) resonance should depend on the

energy, which is effectively higher for $\pi^-$ than for $\pi^+$. To avoid introducing isospin dependence into the quadratic $p$-wave term, we dropped it altogether and made the parameters $c_0$ and $c_1$ complex. Recall that only at the threshold these cannot have imaginary terms. The form of the $s$-wave part of the potential was kept initially as for pionic atoms, while its parameters were also varied in the fit process.

Least-squares fits to the whole $\pi^+$ and $\pi^-$ data together produced reasonably good agreement between calculation and experiment, with $b_0$ and the real parts of $c_0$ and $c_1$ close to the corresponding free $\pi N$ values but with $b_1$ significantly more repulsive than the corresponding free $\pi N$ value of approximately $-0.090m_\pi^{-1}$. The imaginary parts of $c_0$ and $c_1$ were $0.043 \pm 0.009$ and $0.45 \pm 0.11m_\pi^{-3}$, respectively. These must be regarded as effective because they now represent *all* non-$s$-wave absorption processes. The $s$-wave part of the potential which was kept as for pionic atoms showed a factor of 2 reduction in the two-nucleon absorption $\text{Im}B_0$ compared to threshold. This model is denoted below as (a).

With the value of $b_1$ found to be "anomalously" repulsive, as in pionic atoms, we then applied the two mechanisms which have been found to account for that anomaly in the pionic atoms case. The first is that due to Weise [1]: since $b_1$ in free space is well approximated in lowest chiral-expansion order by the Tomozawa-Weinberg expression [22]

$$b_1 = -\frac{\mu_{\pi N}}{8\pi f_\pi^2} = -0.08m_\pi^{-1}, \quad (5)$$

then it can be argued that $b_1$ will be modified in the pion-nucleus interaction if the pion decay constant $f_\pi$ is modified in the medium. The square of this decay constant is given, in leading order, as a linear function of the nuclear density, $f_\pi^{*2} = f_\pi^2 - \rho\sigma/m_\pi^2$, with $\sigma$ the pion-nucleon sigma term. This leads to a density-dependent isovector amplitude such that $b_1$ becomes [3] $b_1(\rho) = b_1(0)/(1 - 2.3\rho)$ for $\sigma = 50$ MeV [23] and with $\rho$ in units of fm$^{-3}$. This model is denoted by (b). The second mechanism which has been successful in pionic atoms is to use the

TABLE I. Results of $\chi^2$ fits to the data using potentials discussed in the text. The $b_1(\rho)$ model is given by $b_1(\rho) = b_1(0)/(1 - 2.3\rho)$. When $b_1$ is complex (bottom half), the listed values refer to its real part.

| Potential model | $b_0$ and $c_0$ | $b_1$ model | $\chi^2$ for 72 points | $b_1(m_\pi^{-1})$ |
|---|---|---|---|---|
| Mixed (a) | Fixed | Fixed | 273 | $-0.125 \pm 0.015$ |
| (b) | | $b_1(\rho)$ | 273 | $-0.098 \pm 0.008$ |
| (c) | $b_0(E)$ and $c_0(E)$ | Fixed | 197 | $-0.117 \pm 0.011$ |
| (d) | | $b_1(\rho)$ | 215 | $-0.087 \pm 0.010$ |
| Linear (a′) | Fixed | Fixed | 309 | $-0.138 \pm 0.010$ |
| (b′) | | $b_1(\rho)$ | 259 | $-0.096 \pm 0.006$ |
| (c′) | $b_0(E)$ and $c_0(E)$ | Fixed | 178 | $-0.134 \pm 0.010$ |
| (d′) | | $b_1(\rho)$ | 214 | $-0.093 \pm 0.007$ |

empirical on-shell energy dependence of the scattering amplitude $b_0$ and scattering volume $c_0$ within the minimal substitution requirement $E \rightarrow E - V_c$ of [9,10] [model (c)]. In additional fits, we have included both mechanisms together [model (d)].

Table I (upper part) summarizes these fits, where "mixed" refers to the model where the $s$-wave term of the potential is of the conventional type, whereas a linear form is used for the $p$-wave part. In the lower part of the table, results are given for fits where the $s$-wave potential, too, was linear; models (a′) to (d′) correspond to models (a) to (d) above, respectively. By replacing the density-quadratic $s$-wave part by a complex linear part, we checked the dependence of the conclusions on the model used, particularly regarding the *in-medium* value of $b_1$, which is found to be essentially decoupled from the rest of the potential.

The obvious conclusions from the table are that (i) without the density dependence of $b_1$, its values differ from the free $\pi N$ value of $-0.090 m_\pi^{-1}$ by $\approx$ 3–4 standard deviations, (ii) with the density dependence included, the values of $b_1$ are in agreement with the free $\pi N$ value, and (iii) the inclusion of the empirical on-shell energy dependence of $b_0$ and $c_0$ leads to improved fits to the data. The solid lines in Fig. 2 show the best fit to the data obtained with the empirical energy dependence within the linear model (c′). Applying also the density dependence of $b_1$ leads to very similar results. The dashed lines show, as an example, results of model (a′) for Ca and it is evident that the agreement with the data is inferior to that achieved with potential (c′), as is also evident from the table. Note that at forward angles there is a limited dependence of the cross sections on the strong interaction potential and the agreement between calculation and experiment essentially proves that the absolute normalization is right. The information on the optical potential comes from larger angles, thus it is the shape of measured angular distributions which is sensitive to the strong interaction. If the data of Wright *et al.* [15] for 19.5 MeV pions scattered from Ca are also included in the analysis, then the resulting potential parameters are unchanged, but their $\pi^-$ cross sections appear to be systematically too small at larger angles by typically 10%.

In conclusion, we have performed precision measurements of elastic scattering of 21.5 MeV positive and negative pions on targets of Si, Ca, Ni, and Zr with the aim of testing the anomalous $s$-wave repulsion observed in pionic atoms. In particular, we focused on the question of whether the mechanisms, which were shown recently to be capable of removing the anomaly in the atomic case, would be required also in the scattering regime in order to reconcile the pion-nucleus interaction with the free pion-nucleon interaction. It is found that (i) the in-medium isovector amplitude $b_1$ is too repulsive by 3–4 standard deviations compared to the free $\pi N$ value and (ii) that including the empirical on-shell energy dependence of the scattering amplitude $b_0$ and the scattering volume $c_0$ improves the fits to the data. However, and *unlike the case with pionic atoms*, the energy dependence alone does *not* remove the extra repulsion. Only with the inclusion of the chiral-motivated model, where the pion decay constant is modified in the medium, it is possible to reconcile the pion-nucleus interaction with the free pion-nucleon interaction, thus removing the anomaly in the isovector channel.

---

*Corresponding author.
Electronic address: elifried@vms.huji.ac.il

[1] W. Weise, Acta Phys. Pol. B **31**, 2715 (2000); Nucl. Phys. **A690**, 98c (2001).

[2] P. Kienle and T. Yamazaki, Phys. Lett. B **514**, 1 (2001).

[3] E. Friedman, Phys. Lett. B **524**, 87 (2002); Nucl. Phys. **A710**, 117 (2002).

[4] E. Friedman and A. Gal, Nucl. Phys. **A721**, 842c (2003).

[5] H. Geissel *et al.*, Phys. Lett. B **549**, 64 (2002).

[6] E. Friedman and A. Gal, Nucl. Phys. **A724**, 143 (2003).

[7] E. E. Kolomeitsev, N. Kaiser, and W. Weise, Phys. Rev. Lett. **90**, 092501 (2003).

[8] E. E. Kolomeitsev, N. Kaiser, and W. Weise, Nucl. Phys. **A721**, 835c (2003).

[9] E. Friedman and A. Gal, Phys. Lett. B **578**, 85 (2004).

[10] T. E. O. Ericson and L. Tauscher, Phys. Lett. B **112**, 425 (1982).

[11] T. Yamazaki *et al.*, Z. Phys. A **355**, 219 (1996).

[12] H. Gilg *et al.*, Phys. Rev. C **62**, 025201 (2000).

[13] H. Geissel *et al.*, Phys. Rev. Lett. **88**, 122301 (2002).

[14] K. Suzuki *et al.*, Phys. Rev. Lett. **92**, 072302 (2004).

[15] D. H. Wright *et al.*, Phys. Rev. C **37**, 1155 (1988).

[16] http://people.web.psi.ch/foroughi/.

[17] B. M. Barnett *et al.*, Nucl. Instrum. Methods Phys. Res., Sect. A **297**, 444 (1990).

[18] C. Joram *et al.*, Phys. Rev. C **51**, 2159 (1995).

[19] M. Ericson and T. E. O. Ericson, Ann. Phys. (N.Y.) **36**, 323 (1966).

[20] C. J. Batty, E. Friedman, and A. Gal, Phys. Rep. **287**, 385 (1997).

[21] G. Burleson *et al.*, Phys. Rev. C **49**, 2226 (1994).

[22] Y. Tomozawa, Nuovo Cimento A **46**, 707 (1966); S. Weinberg, Phys. Rev. Lett. **17**, 616 (1966).

[23] M. E. Sainio, $\pi N$ Newsletter **16**, 138 (2002).